

# Natural human mobility patterns and spatial spread of infectious diseases

Vitaly Belik,<sup>1,2,\*</sup> Theo Geisel,<sup>1,3</sup> and Dirk Brockmann<sup>4,5</sup>

<sup>1</sup>*Max Planck Institute for Dynamics and Self-Organization, Göttingen, Germany*

<sup>2</sup>*Massachusetts Institute of Technology, Department of Civil and Environmental Engineering, Cambridge, MA, USA*

<sup>3</sup>*Institute for Nonlinear Dynamics, Department of Physics, University of Göttingen, Göttingen, Germany*

<sup>4</sup>*Northwestern Institute on Complex Systems, Northwestern University, Evanston, IL, USA*

<sup>5</sup>*Department of Engineering Sciences and Applied Mathematics, Northwestern University, Evanston, IL, USA*

(Dated: October 30, 2018)

We investigate a model for spatial epidemics explicitly taking into account bi-directional movements between base and destination locations on individual mobility networks. We provide a systematic analysis of generic dynamical features of the model on regular and complex metapopulation network topologies and show that significant dynamical differences exist to ordinary reaction-diffusion and effective force of infection models. On a lattice we calculate an expression for the velocity of the propagating epidemic front and find that in contrast to the diffusive systems, our model predicts a saturation of the velocity with increasing traveling rate. Furthermore, we show that a fully stochastic system exhibits a novel threshold for attack ratio of an outbreak absent in diffusion and force of infection models. These insights not only capture natural features of human mobility relevant for the geographical epidemic spread, they may serve as a starting point for modeling important dynamical processes in human and animal epidemiology, population ecology, biology and evolution.

PACS numbers: 89.75.-k, 05.70.Ln, 87.23.Ge, 02.50.Ga, 82.40.Ck

The geographic spread of emergent infectious diseases, epitomized by the 2009 H1N1 outbreak and subsequent pandemic [1], the worldwide spread of SARS in 2003 [2, 3], and recurrent outbreaks of influenza epidemics [4–6], is determined by a combination of disease relevant human interactions and mobility across multiple spatial scales [7]. While infectious contacts yield local outbreaks and proliferation of a disease in single populations, multiscale human mobility is responsible for spatial propagation [8]. Therefore, a prominent lineage of mathematical models has evolved that is based on reaction-diffusion dynamics [9, 10] in which the combination of local exponential growth and diffusive dispersal captures qualitative aspects of observed dynamics. Typically these systems exhibit constant velocity epidemic wavefronts. A related class of phenomenological models is based on the concept of an effective force of infection across distance and thus does not require explicit modelling of dispersal [11, 12].

Although more sophisticated models [2, 4, 13, 14] have been developed to describe the dynamics of recent emergent epidemics such as the H1N1 pandemic or SARS, taking into account long distance travel and multiscale mobility networks [15], the majority of these models are still based on the interplay of local reaction kinetics and diffusion processes on networks of metapopulations. The key assumptions of diffusive transport (Fig.1 (a)) are that a) individuals behave identically, b) movements are stochastic, c) spatial increments are local and as consequence individuals eventually visit every location in the system. Although it is intuitively clear that these assumptions are idealizations in conflict with everyday experience, the

difficulty is how to refine them when data on mobility is lacking, is insufficient or incomplete. Fortunately, a series of recent studies [16–19] substantially advanced our knowledge on multiscale human mobility. An important discovery that emerged from these studies, are individual mobility networks, i.e. individuals typically only visit a limited number of places frequently, predominantly performing commutes between home and work locations and possibly a few other locations. Consequently individuals or groups of individuals exhibit spatially constrained movement patterns despite their potentially high mobility rate. It has remained elusive how this novel and important empirical insight on individual mobility networks can be reconciled with epidemiological models, to which extent it may impact spatial disease dynamics, and how it may alter spreading scenarios and predictions promoted by ordinary reaction-diffusion models, in which mobile hosts can reach every location in the system.

In this Letter we demonstrate how individual mobility networks can be incorporated into a class of models for spatial disease dynamics, and address the questions whether and how significantly the existence of spatially constrained individual mobility networks impact on key features of disease dynamics. To this end we investigate a model that explicitly accounts for bidirectional mobility of individuals between their unique base location (e.g. their home) and a small set of other locations (Fig.1(b)). The entire population is therefore represented by a set of overlapping individual mobility networks associated with each base location, see e.g. [20–22]. We focus on the analysis of epidemics on regular lattices and complex metapopulation networks and systematically compare the dynamics to reaction-diffusion systems as well as force of infection models. In conflict with reaction-diffusion models, in which front velocities increase with

\* e-mail:belik@mit.edu

travel rates unboundedly, we show that our model predicts a saturation of wave front velocities, a direct consequence of the rank of locations in individual mobility patterns. This suggests that estimates for propagation speeds may have been considerably overestimated in the past. Furthermore, we analyze a fully stochastic model to show that both, in regular lattices as well as complex metapopulation networks the global outbreak of a disease is determined by a novel type of threshold for the attack ratio of the disease which depends on the characteristic time spent at distant locations. Finally, we show that in the limit of low and high travel rates our model agrees with reaction-diffusion models and the direct force of infection class of models, respectively.

Consider a system of  $M$  populations labeled  $m$  and assume that in each an epidemic outbreak can be described by a compartmental SIR-model

$$I_m + S_m \xrightarrow{\alpha} 2I_m, \quad I_m \xrightarrow{\beta} R_m, \quad (1)$$

where  $S_m, I_m$  and  $R_m$  label and quantify susceptible, infected and recovered individuals of population  $m$ . Infections and recovery events occur at rates  $\alpha$  and  $\beta$ , respectively, with  $\alpha > \beta$ . The number of individuals in population  $m$  is given by  $N_m = S_m + I_m + R_m$ , which though is conserved only in statistical sense at equilibrium. This system of reactions yields the mean-field description  $\partial_t I = \alpha IS/N - \beta I$  and  $\partial_t S = -\alpha IS/N$ . A natural and plausible extension to a system of  $M$  coupled populations is diffusive dispersal among those populations defined by a hopping rates  $w_{nm} > 0$  from population  $m$  to  $n$ , which yields a metapopulation reaction-diffusion system, i.e. (for infectives and susceptibles)

$$\begin{aligned} \partial_t I_n &= \alpha S_n I_n / N_n^s - \beta I_n + \sum_m (w_{nm} I_m - w_{mn} I_n) \\ \partial_t S_n &= -\alpha S_n I_n / N_n^s + \sum_m (w_{nm} S_m - w_{mn} S_n) \end{aligned} \quad (2)$$

where  $N_n^s$  is the number of individuals in population  $n$  in diffusive equilibrium. Travel rates  $\omega_{mn}$  are usually estimate by gravity-like laws [23].  $N_n^s$  is determined by detailed balance, i.e.  $N_n^s/N_m^s = w_{nm}/w_{mn}$  and conservation of the number of individuals in the metapopulation  $\mathcal{N} = \sum_m N_m^s$ . These type of models have been employed in numerous recent studies [2, 14, 24, 25]. The tight connection to spatially continuous reaction diffusion systems is revealed for the special case of a linear grid of populations placed at regular intervals  $l$  at positions  $x_m = ml$  and mobility between neighboring populations, i.e.  $w_{nm} = \omega \delta_{n-1,m} + \omega \delta_{n+1,m}$  which yields

$$\begin{aligned} \partial_t j &= \alpha j s - \beta j + D \partial_x^2 j \\ \partial_t s &= -\alpha j s + D \partial_x^2 s \end{aligned} \quad (3)$$

in which  $j(x, t) = I_n/N_n^s$ ,  $s(x, t) = S_n/N_n^s$  and  $D = l^2 w$ . Eq. (3) is related to a classic form of a Fisher equation which has been deployed in mathematical epidemiology [9, 10]. For sufficiently localized initial conditions

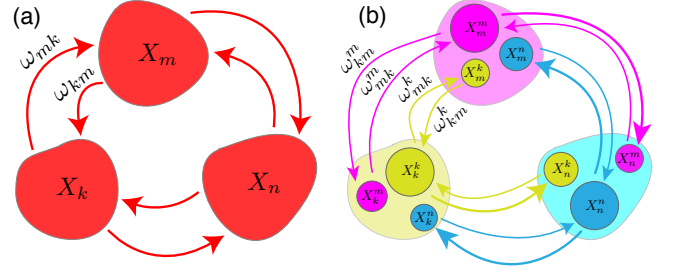


Figure 1. (color online) Metapopulation mobility models. Patches and arrows represent individual populations and travel. (a) Diffusive dispersal: indistinguishable individuals travel randomly between different locations governed by the set of transition rates  $\omega_{nm}$ . (b) Dispersal capturing individual mobility patterns. Individuals with label  $k$  possess travel rates  $\omega_{mk}^k$  and  $\omega_{km}^k$  at which they travel from their base location  $k$  to connected locations  $m$  and back.

this systems exhibits travelling waves with speed

$$c = 2\sqrt{\alpha D(1 - \beta/\alpha)} \sim \sqrt{\omega}. \quad (4)$$

Note that this velocity increases monotonically with the mobility rate  $\omega$ .

In order to account for individual mobility patterns we propose the following generalization: individuals possess two indices  $n$  and  $k$ , characterizing their current and their base location, respectively. The dispersal dynamics is governed by a Markov process

$$X_n^k \xrightleftharpoons[\omega_{nm}^k]{\omega_{mn}^k} X_m^k, \quad (5)$$

where  $X$  stands for each infectious state  $S, I$  and  $R$ . Eqs. (5) imply that individuals with base location  $k$  possess a unique mobility rate  $\omega_{nm}^k$  that determines how they travel between locations  $n$  and  $m$ . This yields a generalization of (2):

$$\begin{aligned} \partial_t I_n^k &= \frac{\alpha}{N_n} S_n^k \sum_m I_n^m - \beta I_n^k + \sum_m (\omega_{nm}^k I_m^k - \omega_{mn}^k I_n^k) \\ \partial_t S_n^k &= -\frac{\alpha}{N_n} S_n^k \sum_m I_n^m + \sum_m (\omega_{nm}^k S_m^k - \omega_{mn}^k S_n^k) \end{aligned} \quad (6)$$

where  $I_n^k$  and  $S_n^k$  are the number of infecteds and susceptibles of type  $k$  that are currently located in population  $n$ .  $N_n$  is the total number of individuals at  $n$ , i.e.  $N_n = \sum_k (I_n^k + S_n^k + R_n^k)$ . If  $\omega_{nm}^k$  are  $k$ -independent, we recover the reaction-diffusion case described above. In the following we consider the case of overlapping star-shaped networks corresponding to commuting between base and destination locations only. This implies that  $\omega_{nm}^k = 0$  if either  $k \neq n$  or  $k \neq m$ . We further assume the constant return rate  $w_{mk}^k = w^-$  for all  $k$  and  $m$ . Realistically we have  $\omega_{kn}^n/\omega^- \ll 1$ , implying individuals belonging to  $n$  remain at their base most of the time.

If mobility rates are large compared to the rates associated with the infection and recovery, i.e.  $\omega_{mk}^k, \omega^- \gg \alpha, \beta$ ,

detailed balance is fulfilled for infecteds and susceptibles separately and the last term in Eq. (6) vanishes in which case the above model is equivalent to the remote force of infection model, see also [11, 21].

In general, it is difficult if not impossible to extract the dynamic differences between the systems defined by Eqs. (2) and (6) for an arbitrary metapopulation. Yet, it is crucial to understand the key dynamic differences that emerge when individual mobility patterns replace ordinary diffusion. We therefore investigate the impact of individual mobility patterns in the instructive one-dimensional lattice case. We assume that only infecteds can travel and that recovery is absent (SI model), i.e.  $\beta = 0$  (relaxing these two restrictions does not change the main results but clarifies the analysis). We denote the number of infecteds with base location  $n$  that are located on site  $n$  (i.e. their base) and sites  $n \pm 1$  by  $I_n^n$  and  $I_n^{\pm}$ , respectively. At rates  $\omega^+$  and  $\omega^-$  individuals leave and return to their base. In order to obtain a spatially continuous description we approximate  $I_{n\pm 1}^{\pm} \rightarrow I^{\pm}(x \pm l) \approx I^{\pm} \pm l \nabla I^{\pm} + \frac{l^2}{2} \Delta I^{\pm}$  and introduce relative concentrations  $u_n = I_n/N$ ,  $v_n = (I_n^+ + I_n^-)/N$  leading to

$$\begin{aligned} \partial_t u &= \alpha(1 - u - v)(u + v + \mathcal{D}\Delta v) + \omega^- v - 2\omega^+ u \\ \partial_t v &= 2\omega^+ u - \omega^- v \end{aligned} \quad (7)$$

where  $\mathcal{D} = l^2/2$ . The function  $u(x, t)$  is the fraction of individuals based and located at  $x$  whereas  $v(x, t)$  is the fraction of individuals based but not located at  $x$ . Note that we discarded here a third equation for  $w = (I^+ - I^-)/N$  independent from (7) with a solution vanishing at long times. This does not change the main result (8). The non-trivial steady state is given by  $u^* = \omega^-/(2\omega^+ + \omega^-)$ ,  $v^* = 2\omega^+/(2\omega^+ + \omega^-)$  with  $u^* + v^* = 1$  as expected.

One of the key questions is if the system (7) exhibits stable propagating waves as solutions and how their velocity depends on system parameters. The ansatz  $u(x, t) = \tilde{u}(x - ct)$  and likewise for  $v$ , leads to a stable solution with a velocity given by

$$c = \frac{2\alpha\omega^+ \sqrt{\mathcal{D}(2 + \omega^-/\omega^+)}}{(\alpha + \omega^- + 2\omega^+)}. \quad (8)$$

Fixing  $\omega^-$  this implies that  $c \rightarrow 0$  as  $\omega^+ \rightarrow 0$ . On the other hand if  $\omega^-$  is small, the system is entirely determined by forward rate  $\omega^+$ . For a systematic comparison to the ordinary reaction-diffusion system, we have to establish a relation between  $\omega^{\pm}$  and  $\omega$  in Eq. (4). For the sake of simplicity we consider the symmetric case, i.e.  $\omega^+ = \omega^- = \omega$ , yielding

$$c = \frac{2\sqrt{6\mathcal{D}}\alpha\omega}{(\alpha + 3\omega)}. \quad (9)$$

Numerical simulations of a fully stochastic system nicely agree with the analytical predictions (Fig. 2). The essential feature of  $c(\omega)$  is its saturation as  $\omega \rightarrow \infty$  whereas

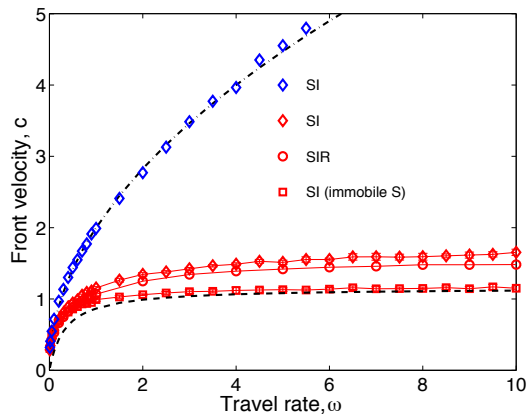


Figure 2. (color online) Front velocity  $c(\omega)$  of the model defined by Eq. (6) as a function of mobility rate  $\omega$  in comparison to ordinary reaction-diffusion dynamics (Eq. (2)). For stochastic simulations we used a lattice with  $10^2$  sites and  $N = 10^4$  individuals/site. Mean velocities are indicated by red (bi-directional mobility) and blue (reaction-diffusion) symbols. Analytical results, i.e. Eqs. (9) and (4) are shown by dashed and dash-dotted lines respectively.

$c \sim \sqrt{\omega}$  for reaction-diffusion systems. This effect is a direct consequence of the spatial constraints imposed by individual mobility patterns, i.e. increasing the mobility rate  $\omega$  yields a higher frequency of travel events but restricted to the set of locations connected to the base location and thus is universal and holds also for more complex metapopulation topologies [26]. For high rates the deviation between ordinary reaction diffusion and bi-directional mobility increases without bounds. This is an important insight as the expression for wave front speeds for reaction-diffusion have been used in the past to estimate wave front speeds from mobility rates and vice versa. Our results indicate that if constrained mobility patterns and bi-directional movement patterns are at work these estimates must be treated with particular care. Note that in the limit  $\omega \rightarrow \infty$  Eq. (7) reduces to the heuristic equation in Ref. [27].

A key question in epidemiological contexts concerns conditions under which an epidemic outbreak propagates or wanes. Outbreak dynamics is usually triggered by crossing thresholds inherent in the system's dynamics [28]. For example the basic reproduction number  $\mathcal{R}_0$  of a disease, i.e. the expected number of secondary cases caused by a single infected individual in a susceptible population represents such a threshold [8]. In single population SIR dynamics introduced above  $\mathcal{R}_0 = \alpha/\beta$ . If  $\mathcal{R}_0 > 1$  an outbreak occurs, otherwise epidemic dies out. In the extended metapopulation system with diffusive host movements a second threshold, known as the global invasion threshold [24], is induced by the flux of individuals between populations which must be sufficiently high for an epidemic to spread throughout the metapopulation.

An interesting and important feature of the model we

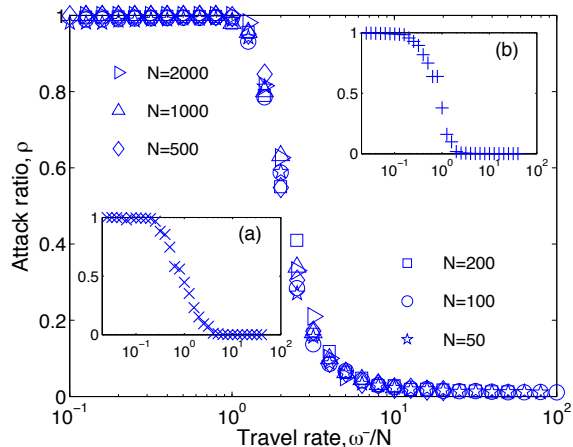


Figure 3. Results of stochastic simulations. Attack ratio  $\rho(\omega^-/N)$  as a function of the return travel rate  $\omega^-$  for SIR epidemics on a lattice with  $10^2$  sites with  $N$  agents/site. Epidemic parameters:  $\alpha = 1$ ,  $\beta = 0.1$ . Insets: (a) —  $\rho(\omega^-/N)$  for a scale-free network ( $\gamma = 1.5$ ) of  $10^3$  nodes populated uniformly with  $\langle N \rangle = 250$ /site, with  $k_{\min} = 5$  and  $k_{\max} = 50$ ; (b) —  $\rho(\omega^-/N)$  for an Erdős-Rényi network with 500 nodes and  $\bar{k} = 10$ . Results were averaged over 50 realisations. Interlocation flux rate was  $\langle \omega \rangle = 1$ .

propose is the existence of another invasion threshold which is determined by the return rate  $\omega^-$  or equivalently by the time an individual spends outside the base location. This finding is illustrated in Fig. 3 which depicts the attack ratio  $\rho$  as a function of  $\omega^-$  for a bidirectional SIR epidemic on a lattice. The attack ratio  $\rho$  is defined as the fraction of the overall population affected during an epidemic. We fixed the entire interlocation flux at a value above the global invasion threshold ensuring global outbreak in the reaction-diffusion system.

This result is universal for bidirectional system and is independent of the particular topology. Insets (a) and (b) of Fig. 3 display simulation results for uncorrelated scale-free and Erdős-Rényi networks. For low return rates the attack ratio is close to unity. However, with growing values of the return rate, the attack ratio decreases steeply and vanishes, reflecting the absence of the global outbreak. The regime of high return rates corresponds to small dwelling times on distant locations. Infected individuals do not have enough time to transfer the disease to susceptibles in unaffected locations before they return. Note that for a wide range of local population sizes (50 – 2,000) the attack ratio  $\rho$  collapses onto a universal curve  $\rho \sim \rho(\omega^-/N)$  which suggests that the basic mechanism of the invasion threshold and its functional dependence on return rate  $\omega^-$  can be understood theoretically.

To estimate the observed invasion threshold on a one-dimensional lattice for  $\mathcal{R}_0 \gtrsim 1$  we calculated the number of infecteds  $\lambda$  that originate from an affected location and can seed an outbreak in an unaffected one [28]. These

seeders are approximately given by the total number of individuals entering the new location per unit time, i.e.  $N\omega$  multiplied by the typical time they remain active in the destination location. This time is given by the inverse rate  $r$  of exiting the seeders class. Since two processes (returning to the base location and recovery) can trigger this exit,  $r = \beta + \omega^-$ . Therefore  $\lambda \approx N\omega/(\beta + \omega^-)$ . In the tree approximation the threshold condition for an epidemic on a network with an average degree  $\bar{k}$  is given by  $\lambda(\bar{k} - 1)(\mathcal{R}_0 - 1) > 1$  [24]. Thus, for a one-dimensional lattice the threshold condition reads

$$\frac{\omega^-}{\beta} \lesssim \left( 2N(\mathcal{R}_0 - 1) \frac{\omega^+}{\beta} - 1 \right), \quad (10)$$

where we kept the total interlocation flux  $\omega = 2\omega^+\omega^-/(2\omega^+ + \omega^-)$  constant (this relation and positivity of travel rates impose the restrictions:  $\omega^- > \omega$  and  $\omega^+ < \omega/2$ ) and used  $\omega^+ \ll \omega^-$ . Moreover, as extensive simulations show, the global invasion threshold in terms of the flux rate  $\omega$  exists in bidirectional systems only for low return rates  $\omega^-$ . With increasing return rate the disease fails to propagate globally, even for constant interlocation flux  $\omega$ . This effect, observed in lattice topologies and paradigmatic more realistic network topologies is a fundamental consequence of birectional mobility patterns. This effect is absent in reaction-diffusion systems fully determined by the total interlocation flux. This property implies that invasion of a front is limited only by return rates and not as is typically assumed by the overall particle flux  $\omega$ . In the context of disease dynamics this implies that more efficient containment strategies could be potentially devised that do not target the overall mobility but rather modifies mobility patterns in an asymmetric way.

Note that the transition takes place only in a system with a finite number of agents per site, in the system with an infinite number of individuals this effect would disappear as also confirmed in Fig. 3. Indeed from Eq. (10) for  $\beta \ll \omega^-$  the scaling  $\rho \sim \rho\left(\frac{N\omega}{\omega^-}\right)$  follows — with increasing number of individuals per site  $N$ , the threshold value of the return rate  $\omega^-$  increases.

Recently an unprecedented amount of detailed information on human activity became available requiring revision of established models and new more sophisticated ones. We investigate an epidemiological model explicitly incorporating such important properties of human mobility as individual mobility networks and frequent bidirectional movements between home and destination locations. It manifests surprising dynamical features such as the existence of bounded front velocity and novel propagation threshold which are universal for any metapopulation topology. As more detailed data continues to become available our approach is a promising foundation for the further research.

D.B. and V.B. acknowledge support from the Volkswagen Foundation, D.B. acknowledges EU-FP7 grant Epiwork. V.B and D.B would like to thank W. Noyes, and H. Schlämmer for invaluable comments.

- 
- [1] Christophe Fraser, Christl A Donnelly, Simon Cauchemez, *et al.*, “Influenza: Making privileged data public response,” *Science*, **325**, 1072–1073 (2009).
- [2] L Hufnagel, D Brockmann, and T Geisel, “Forecast and control of epidemics in a globalized world,” *Proc. Natl. Acad. Sci. USA*, **101**, 15124 (2004).
- [3] Vittoria Colizza, Alain Barrat, Marc Barthelemy, *et al.*, “Predictability and epidemic pathways in global outbreaks of infectious diseases: the sars case study,” *BMC Med.*, **5**, 34 (2007).
- [4] D. Balcan, H Hu, B Goncalves, *et al.*, “Seasonal transmission potential and activity peaks of the new influenza A(H1N1): a Monte Carlo likelihood analysis based on human mobility,” *BMC Med.*, **7**, 45 (2009).
- [5] D Balcan, B Goncalves, H Hu, *et al.*, “Modeling the spatial spread of infectious diseases: The GLObal Epidemic and Mobility computational model,” *J. Comp. Sci.*, **1**, 132 (2010).
- [6] D Balcan, V Colizza, B Goncalves, *et al.*, “Multiscale mobility networks and the spatial spreading of infectious diseases,” *Proc. Nat. Acad. Sci. USA*, **106**, 21484 (2009).
- [7] S Riley, “Large-scale spatial-transmission models of infectious disease,” *Science*, **316**, 1298 (2007).
- [8] R M Anderson and R M May, *Infectious Diseases of Humans* (Oxford University Press, 1991).
- [9] A Kolmogorov, I Petrovsky, and N Piscounov, “Étude de l’équation de diffusion avec croissance de la quantité de matière et son application à un problème biologique,” *Bull. de l’univ. d’état à Moscou, Sér. internat., sect. A*, **1**, 1 (1937).
- [10] R A Fisher, “The wave of advance of advantageous gene,” *Ann. Eugenics*, **7**, 355–369 (1937).
- [11] S Rushton and A J Mautner, “The deterministic model of a simple epidemic for more than one community,” *Biometrika*, **42**, 126–132 (1955).
- [12] T J Hagenaas, C A Donnelly, and N M Ferguson, “Spatial heterogeneity and the persistence of the infectious diseases,” *J. Theor. Biol.*, **229**, 349 (2004).
- [13] L A Rvachev and I M Longini, “A mathematical model for the global spread of influenza,” *Math. Biosci.*, **75**, 3 (1985).
- [14] V. Colizza, R. Pastor-Satorras, and A. Vespignani, “Reaction-diffusion processes and metapopulation models in heterogeneous networks,” *Nat. Phys.* (2007).
- [15] Alessandro Vespignani, “Predicting the behavior of techno-social systems,” *Science*, **325**, 425 (2009).
- [16] D Brockmann, L Hufnagel, and T Geisel, “The scaling laws of human travel,” *Nature (London)*, **439**, 462 (2006).
- [17] Marta C González, César A Hidalgo, and Albert-László Barabási, “Understanding individual human mobility patterns,” *Nature (London)*, **453**, 779 (2008).
- [18] Chaoming Song, Zehui Qu, Nicholas Blumm, and Albert-László Barabási, “Limits of predictability in human mobility,” *Science*, **327**, 1018 (2010).
- [19] Chaoming Song, Tal Koren, Pu Wang, *et al.*, “Modelling the scaling properties of human mobility,” *Nat. Phys.*, **6**, 818 (2010).
- [20] Lisa Sattenspiel and Klaus Dietz, “A structured epidemic model incorporating geographic mobility among regions,” *Math. Biosci.*, **128**, 71 (1995).
- [21] Matt J. Keeling and Pejman Rohani, “Estimating spatial coupling in epidemiological systems: a mechanistic approach,” *Ecol. Lett.*, **5**, 20–29 (2005).
- [22] J Arino and P van den Driessche, “The basic reproduction number in a multi-city compartmental epidemic model,” *Lect. Notes in Control and Information Science*, **294**, 135 (2003).
- [23] V V Belik and D Brockmann, “Accelerating random walks by disorder,” *New J. Phys.*, **9**, 54 (2007).
- [24] Vittoria Colizza and Alessandro Vespignani, “Invasion threshold in heterogeneous metapopulation networks,” *Phys. Rev. Lett.*, **99**, 148701 (2007).
- [25] N M Ferguson, D A Cummings, C Fraser, *et al.*, “Strategies for containing an emerging influenza pandemic in Southeast Asia,” *Nature (London)*, **437**, 209 (2005).
- [26] We assume here that individuals return to their base location  $k$  before travelling somewhere else. The initial model defined by Eqs. (5) allows to explore more general mobility patterns by relaxing this assumption. However, as long as the individual rates  $\omega_{nm}^k$  are dominated by the dynamics that incorporate a base location, propagation speeds do not deviate significantly from the model we investigate here.
- [27] U Naether, E B Postnikov, and I M Sokolov, “Infection fronts in contact disease spread,” *Eur. Phys. J. B*, **65**, 353 (2008).
- [28] F Ball, D Mollison, and G Scalia-Tomba, “Epidemics with two levels of mixing,” *Ann. Appl. Prob.*, **7**, 46 (1997).